

THE DISK POPULATION OF THE UPPER SCORPIUS ASSOCIATION¹K. L. LUHMAN^{1,2} AND E. E. MAMAJEK^{3,4}*Draft version June 21, 2018*

ABSTRACT

We present photometry at 3–24 μm for all known members of the Upper Scorpius association ($\tau \sim 11$ Myr) based on all images of these objects obtained with the *Spitzer Space Telescope* and the *Wide-field Infrared Survey Explorer*. We have used these data to identify the members that exhibit excess emission from circumstellar disks and estimate the evolutionary stages of these disks. Through this analysis, we have found ~ 50 new candidates for transitional, evolved, and debris disks. The fraction of members harboring inner primordial disks is $\lesssim 10\%$ for B–G stars ($M > 1.2 M_{\odot}$) and increases with later types to a value of $\sim 25\%$ at $\gtrsim M5$ ($M \lesssim 0.2 M_{\odot}$), in agreement with the results of previous disk surveys of smaller samples of Upper Sco members. These data indicate that the lifetimes of disks are longer at lower stellar masses, and that a significant fraction of disks of low-mass stars survive for at least ~ 10 Myr. Finally, we demonstrate that the distribution of excess sizes in Upper Sco and the much younger Taurus star-forming region ($\tau \sim 1$ Myr) are consistent with the same, brief timescale for clearing of inner disks.

Subject headings: accretion disks — planetary systems: protoplanetary disks — stars: formation — stars: low-mass, brown dwarfs — stars: pre-main sequence

1. INTRODUCTION

Identifying the stars that harbor circumstellar disks within young clusters and associations is an essential step in using disks to study star and planet formation. For instance, thorough surveys for disks provide well-defined samples of targets for detailed measurements of disk properties. In addition, by comparing the prevalence of disks in different evolutionary stages within a given cluster and among clusters across a range of ages, one can estimate the lifetimes and clearing timescales of disks, which in turn constrain models of disk evolution and planet formation.

The best available tool for disk surveys has been mid-infrared (IR) imaging with the *Spitzer Space Telescope* (Werner et al. 2004). *Spitzer* has offered the sensitivity to detect the photospheres of young brown dwarfs in nearby clusters ($d < 500$ pc), the field of view to efficiently map these clusters ($\sim 5'$), the angular resolution to resolve most of their members ($\sim 2''$), and a suite of mid-IR filters that could roughly classify the evolutionary stages of disks (3.6–24 μm). Although *Spitzer* has focused on relatively compact clusters ($\sim 1 \text{ deg}^2$, Lada et al. 2006; Sicilia-Aguilar et al. 2006; Dahm & Hillenbrand 2007; Hernández et al. 2007; Luhman et al. 2008; Gutermuth et al. 2009), it has also imaged more widely distributed populations in areas as large as $\sim 50 \text{ deg}^2$ (Evans et al. 2009; Rebull et al. 2010).

The Upper Scorpius subgroup in the Scorpius-Centaurus OB association is an attractive target for disk surveys. It contains one of the nearest and richest pop-

ulations of young stars ($d = 125\text{--}165$ pc, $N \sim 800$, Preibisch & Mamajek 2008), making it possible to measure disk properties down to low stellar masses with good statistical accuracy. Perhaps most importantly, Upper Sco is at an age where both primordial disks and second-generation debris disks are abundant (Carpenter et al. 2009), and thus can potentially provide vital constraints on disk evolution. Most studies have adopted a mean age of 5 Myr for Upper Sco (de Geus et al. 1989; Preibisch et al. 2002), but Pecaute et al. (2012) recently derived a significantly older value of 11 Myr, which affects the timescales of disk evolution derived from any census of disks in the region. The ages of Upper Sco and its neighboring subgroups remain a subject of debate (Song et al. 2012).

Spitzer has been used to identify and classify disks in Upper Sco based on mid-IR photometry (Carpenter et al. 2006, 2009; Chen et al. 2005, 2011; Riaz et al. 2009) and to study the mineralogy of dust in those disks with mid-IR spectroscopy (Scholz et al. 2007; Dahm & Carpenter 2009). In one of the most widely-cited results from the *Spitzer* data, Carpenter et al. (2006) found that, in a sample of ~ 200 members, nearly all of the stars more massive than the Sun have lost their primordial disks while a significant fraction of the low-mass stars ($\sim 1/5$) have retained them, indicating that disk lifetimes may be longer at lower stellar masses. However, because Upper Sco is spread across a large area ($\sim 100 \text{ deg}^2$), *Spitzer* imaged members individually rather than through a map of the association, and only a subset of the stellar population was observed. As a result, the potential of the association for constraining the properties of disks was not fully exploited.

The *Wide-field Infrared Survey Explorer* (*WISE*, Wright et al. 2010) has presented an opportunity to significantly improve the census of disks in Upper Sco. In 2010, the satellite imaged the entire sky at 3.4, 4.6, 12, and 22 μm , providing mid-IR photometry for the areas

¹ Department of Astronomy and Astrophysics, The Pennsylvania State University, University Park, PA 16802; kluhman@astro.psu.edu.

² Center for Exoplanets and Habitable Worlds, The Pennsylvania State University, University Park, PA 16802.

³ Cerro Tololo Inter-American Observatory, Casilla 603, La Serena, Chile

⁴ On leave, Department of Physics and Astronomy, The University of Rochester, Rochester, NY 14627.

of Upper Sco that were not observed by *Spitzer*. Although they have lower sensitivity and angular resolution than *Spitzer* images, the *WISE* data do detect every known member of Upper Sco (that is resolved) in the most sensitive bands, including the brown dwarfs. *WISE* photometry has already been used to search for disks around members of Upper Sco at B, A, and F types (Rizzuto et al. 2012) and mid- to late-M types (Riaz et al. 2012).

To obtain the most thorough census of disks in Upper Sco that is possible with available data, we have compiled all photometry between 3–24 μm from both *Spitzer* and *WISE* for all known members of the association (Section 2). We use these data to identify the members that exhibit significant mid-IR excesses (Section 3) and to estimate the evolutionary stages of the detected disks (Section 4). We then measure the distribution of excesses as a function of spectral type, wavelength, disk class, and excess size and discuss the resulting implications for disk evolution (Section 5).

2. DATA FOR UPPER SCO

2.1. Known Members

To characterize the population of disks in Upper Sco, we began by constructing a list of all published sources that are likely to be members of the association based on proper motions or diagnostics of youth. We also have included new members that we have uncovered through an ongoing survey of the association. The basis for inclusion in our membership catalog will be described in a separate study (K. Luhman, in preparation). We have treated known binaries as single sources if they are unresolved by both the Two Micron All-Sky Survey (2MASS, Skrutskie et al. 2006) and the United Kingdom Infrared Telescope (UKIRT) Infrared Deep Sky Survey (UKIDSS, Lawrence et al. 2007)⁵. Thus, secondaries that have been resolved only by high-resolution imaging with the *Hubble Space Telescope* or adaptive optics do not receive separate entries in our catalog of members (Luhman 2005; Kraus et al. 2005; Lafrenière et al. 2008, 2011; Biller et al. 2011; Ireland et al. 2011). Our resulting list of known members of Upper Sco contains 863 objects. We present their names and spectral types in Table 1. Our compilation of spectral classifications is not fully exhaustive; additional measurements have been reported in the literature for some of the stars, particularly at earlier types, but they generally agree with the types in Table 1.

2.2. *Spitzer* Photometry

For our census of disks in Upper Sco, we make use of images at 3.6, 4.5, 5.8, and 8.0 μm obtained with *Spitzer*'s Infrared Array Camera (IRAC; Fazio et al. 2004) and images at 24 μm obtained with the Multiband Imaging Photometer for *Spitzer* (MIPS; Rieke et al. 2004). These bands are denoted as [3.6], [4.5], [5.8], [8.0], and [24]. The fields of view were $5'2 \times 5'2$ and $5'4 \times 5'4$ for IRAC and

the 24 μm band of MIPS, respectively. The cameras produced images with FWHM = $1''.6$ – $1''.9$ from 3.6 to 8.0 μm and FWHM = $5''.9$ at 24 μm .

Several previous studies have reported *Spitzer* photometry for samples of members of Upper Sco (Rieke et al. 2005; Chen et al. 2005; Padgett et al. 2006; Carpenter et al. 2006, 2008, 2009; Scholz et al. 2007; Riaz et al. 2009). In this work, we consider all IRAC and MIPS 24 μm observations of all members in our catalog. These data were obtained through Guaranteed Time programs 19 (J. Houck), 40, 58 (G. Rieke), 72 (F. Low), and 84 (M. Jura), Director's Discretionary Time program 248 (S. Mohanty), Legacy programs 139, 173, 177 (N. Evans), 148 (M. Meyer), and 30574 (L. Allen), and General Observer programs 20069 (J. Carpenter), 20103 (L. Hillenbrand), 20146 (K. Gordon), 20435 (R. Jayawardhana), 20803 (S. Mohanty), 30765 (K. Stapelfeldt), 50025 (P. Harvey), 50554 (I. Song), and 80187 (K. Luhman). We have measured photometry from these images for the members of Upper Sco with the methods described by Luhman et al. (2010).

We present our measurements of *Spitzer* photometry for Upper Sco in Table 1. Some members were observed at multiple epochs, most of which were separated by a few days. Since none of these objects exhibit significant variability in these data, we report the mean of multiple measurements weighted by the inverse square of their flux errors. For each of the IRAC bands, the camera detected every member that appeared within the field of view and was resolved. This was not the case for the 24 μm images from MIPS. All of the non-detections in this band are indicated in Table 1. The typical detection limit is $[24] \sim 10$. We have not measured 24 μm photometry for HIP 80425 and HIP 80338 since they are dominated by extended emission. 2MASS J16105240-1937344 also may be significantly contaminated by extended emission at 24 μm . We report a tentative measurement for this star, but it is excluded from the analysis in this paper. Carpenter et al. (2009) noted that their 24 μm data for several additional stars were unreliable because of extended emission. Based on visual inspection of the images, we find that these stars are point sources that are sufficiently bright compared to spatial variations in the background emission so that our aperture photometry should be reasonably accurate. This conclusion is supported by the fact that our 24 μm data for these stars agree with the fluxes expected from the photospheres. IRAC and MIPS observed 381 and 442 members of Upper Sco, respectively. A total of 484 members were observed by at least one of the cameras, corresponding to 56% of the known members. IRAC and MIPS data have not been previously published for 117 and 124 of these sources, respectively, which includes 48 non-detections by MIPS.

2.3. *WISE* Photometry

In addition to the pointed *Spitzer* observations, we utilize mid-IR photometry from the all-sky imaging survey by *WISE*. The bands of *WISE* are centered at 3.4, 4.6, 12, and 22 μm , which are denoted as W1 through W4 (Wright et al. 2010). The angular resolution of the *WISE* images is $\sim 6''$ in the first three bands and $\sim 12''$ in W4.

We have retrieved the coordinates and profile-fit photometry of all objects in the *WISE* Preliminary Release

⁵ UKIDSS uses the UKIRT Wide Field Camera (WFCAM, Casali et al. 2007) and a photometric system described by Hewett et al. (2006). The pipeline processing and science archive are described by Irwin et al. (in preparation) and Hambly et al. (2008).

Source Catalog and the *WISE* All-Sky Source Catalog that are within a distance of $3''$ from members of Upper Sco. For W1 and W2, most of the data agree within 5% between the two catalogs, and the catalogs exhibit comparable agreement with the *Spitzer* data. The width of the sequence of diskless stars in $K_s - W1$ and $K_s - W2$ as a function of spectral type is also similar for the two catalogs (Section 3). We adopt the W1 and W2 data from the All-Sky Source Catalog since it was generated from a newer processing of the *WISE* images. However, we find that the sequences of diskless stars in $K_s - W3$ and $K_s - W4$ are noticeably tighter with the data from the Preliminary Release Source Catalog for the fainter stars, which implies better photometric accuracies in this catalog for W3 and W4. This result is supported by a comparison of W4 to our measurements of [24]; the standard deviation of $W4 - [24]$ is 0.18 and 0.28 mag using the Preliminary Release and All-Sky data, respectively. Therefore, we adopt the W3 and W4 measurements from the Preliminary Release Source Catalog, with the exception of 2MASS J16045716-2104160, 2MASS J16133647-2327353, and 2MASS J16133688-2327298, for which measurements are available from only the All-Sky Source Catalog. On average, the data from the Preliminary Release Source Catalog for Upper Sco are 0.03 mag brighter in W3 and 0.035 mag fainter in W4 than the data from the All-Sky Source Catalog.

We have modified our catalog of *WISE* data in several ways. Since the W2 fluxes for saturated stars are significantly overestimated (0.2–1 mag at $W2 < 6$, Cutri et al. 2012), we have omitted these measurements from our tabulation. These empty entries in the catalog are labeled with the flag “err”. Biases of this kind are also present in the other bands for the brightest stars, but they are much smaller ($\lesssim 0.2$ mag), so we retain these measurements. Although the All-Sky Source Catalog contains data for Antares, we label it as saturated in our catalog since it is too bright for reliable photometry. Through visual inspection of the *WISE* images, we have checked for members of Upper Sco whose *WISE* photometry may be affected by the PSF of another star. Each band in which this occurs is labeled with the flag “bl” (for “blend”). We also have inspected the images to check for unreliable detections and measurements that may be contaminated by extended emission. For the former, we have omitted the *WISE* photometry and have added the flag “false” to our catalog. The *WISE* photometry is labeled with the flag “ext” if extended emission is suspected based on the visual inspection. If measurements are known to be dominated by extended emission based on higher-resolution images from *Spitzer*, they are omitted from the catalog. Some studies have excluded data that have high values of the reduced χ^2 for the profile fitting in the *WISE* catalog because this may indicate the presence of extended emission (Rizzuto et al. 2012). However, we find that most of the members of Upper Sco with high χ^2 do not show evidence of extended emission in images from *Spitzer*, when available. Therefore, we rely on the steps that we have described rather than the χ^2 flag for identifying extended emission. Finally, for the source in the *WISE* catalog matched to each member, we have visually checked whether its position differs significantly ($\gtrsim 2''$) among the four *WISE* bands. By doing so, we can identify erroneous matches in the *WISE* catalog between

one object that dominates at shorter wavelengths and a different object that dominates at longer wavelengths, as in the case of the components of a binary system in which only the secondary has a disk (e.g., 2MASS J16101888-2502325 and 2MASS J16101918-2502301) and stars and red galaxies with small projected separations (e.g., Sco PMS 17, Carpenter et al. 2009).

We have examined the *WISE* images of all members that lack counterparts in the *WISE* catalog. Several of the unmatched members are not detected because of their proximity to brighter stars. We label their empty entries with the flag “unres”. Among the pairs separated by less than $6''$ (the FWHM for the shorter bands), we have attached “bin” (for “binary”) to the photometry of the brighter components to indicate a possible contribution from the fainter stars. As noted in Section 2.1, many known close companions are not included in our catalog of members. Thus, they represent additional unresolved components in the *WISE* data that are not marked in our catalog. Finally, through visual inspection of the images, we find that *WISE* did detect four members that are absent from the Source Catalogs. We found data for two of these stars, 2MASS J16071750-1820348 and 2MASS J16001730-2236504, in the *WISE* All-Sky Reject Table. We measured photometry for the remaining stars, 2MASS J16090407-2417588 and 2MASS J16081758-2348508, by applying aperture photometry to the *WISE* images. We present our catalog of *WISE* photometry for the known members of Upper Sco in Table 1.

3. MEASUREMENT OF INFRARED EXCESS EMISSION

A dusty circumstellar disk within a few AU of a star is brightest at IR wavelengths, becoming brighter than the star beyond $\sim 5 \mu\text{m}$. As a result, one can detect the presence of a disk based on IR emission that is greater than that expected from a stellar photosphere. We have applied this technique to the *Spitzer* and *WISE* photometry in Upper Sco to identify the members that have disks. To detect and measure excess emission for each member, we have used the colors produced by the *Spitzer* and *WISE* bands relative to K ($2.2 \mu\text{m}$). We use K for these colors because it is long enough in wavelength so that extinction is low while short enough in wavelength that it is usually dominated by the stellar photosphere in systems with disks. For most stars, we adopt K_s from the 2MASS Point Source Catalog or K from the seventh data release of UKIDSS, whose photometric systems are similar (Hodgkin et al. 2009). We use K photometry from The et al. (1986) and Kimeswenger et al. (2004) for a few of the brightest members since their 2MASS data have large uncertainties. We focus on the *Spitzer* bands [4.5], [8.0], and [24] and the *WISE* bands W2, W3, and W4 for detecting excess emission. We do not consider [3.6] and W1 since they should show the smallest excesses among the *Spitzer* and *WISE* bands. The data at [5.8] is discussed only briefly since it is available for a relatively small number of members. Antares is excluded from our analysis since it is a red supergiant and it lacks data from *Spitzer* or *WISE*.

The color excess of a star is measured by comparing its observed color to the color expected for its stellar photosphere. Because of its richness and moderately advanced age, Upper Sco contains a large number of diskless stars, providing an accurate determination of

the colors of young photospheres. Since photospheric colors can vary with spectral type, we plot the IR colors in Upper Sco as a function of spectral type in Figure 1. The colors are not corrected for extinction, which is typically $A_V = 1\text{--}2$ in this association. We have indicated in Figure 1 the known and suspected Be stars (Merrill & Burwell 1933; Jaschek et al. 1964; Crampton 1968; Coté & van Kerkwijk 1993; Cieza et al. 2010) and the candidates for disks in different evolutionary classes that are identified in Section 4 and in previous studies (Cieza et al. 2007; Carpenter et al. 2009; Chen et al. 2006, 2011). For each color in Figure 1, the data exhibit a narrow sequence of blue sources and a broader distribution of redder sources, corresponding to stellar photospheres and stars with disks, respectively. We discuss the measurement of excesses from these colors in the remainder of this section. The results of this analysis are summarized in Table 1, where we indicate whether each member of Upper Sco has excess emission in each of the six *Spitzer* and *WISE* bands that we have considered.

3.1. Excesses in [4.5] and W2

We examine the data in [4.5] and W2 together since these bands have similar effective wavelengths (4.5 and 4.6 μm). Photometry in [4.5] and W2 is available for 359 and 817 members of Upper Sco, respectively. The stars that lack [4.5] were not observed by IRAC while the stars that lack W2 are too bright for good photometry (Section 2.3) or are blended with other sources. Thus, all members were detected in both bands as long as they were observed (by IRAC) and resolved. 26 members have [4.5] but not W2, which consist of stars that are too bright for a reliable W2 measurement and companions that are resolved by IRAC but not *WISE*. As a result, 843 members have data in at least one of the two bands.

In the diagrams of $K_s - [4.5]$ and $K_s - W2$ versus spectral type in Figure 1, we have used the sequences of diskless stars to select boundaries for identifying stars that exhibit significant color excesses. We use the same boundary for both colors since the data in [4.5] and W2 have an average offset of less than a few percent. However, the photospheric sequences are not well-defined at the latest spectral types because of the small number of members. The bluest L-type members have colors near 1.2, which is redder than the photospheric values of $K_s - [4.5]$ estimated by Luhman et al. (2010) based on young L dwarfs in the solar neighborhood ($\tau \sim 10\text{--}100$ Myr). To better define the photospheric colors for L-type members of Upper Sco, we include in Figure 1 data for members of Taurus that are later than M9 and that are diskless based on photometry at longer wavelengths (Luhman et al. 2010). These data coincide with the bluest sources in Upper Sco and confirm the rapid increase in $K_s - [4.5]$ and $K_s - W2$ beyond M9. The boundaries for $K_s - [4.5]$ and $K_s - W2$ are defined by lines connecting (B0, 0.19), (K0, 0.22), (M1.5, 0.47), and (M8.5, 0.87). Since the dependence on spectral type of these colors remains somewhat uncertain at M9–L2, we end the boundaries in Figure 1 at M8.5. Measurements of excesses at the latest types are also sensitive to uncertainties in spectral types because of the rapid increase in the photospheric colors. Nevertheless, we have inspected the data to check for members later than M8.5 that show obvious excesses. [LHJ2006] J163919.15-253409.9 has an

excess in W2 but not [4.5]. This discrepancy is a reflection of the fact that W2 is brighter than [4.5] by 0.35 mag. A similar offset is present between W1 and [3.6], indicating that the source is variable. [LHJ2007] J160918.69-222923.7 exhibits the same characteristics. Mid-IR variability of this size is more likely to occur in stars with disks (Luhman et al. 2008, 2010). Therefore, we classify these two objects as having excesses in W2. We tentatively conclude that the remaining members later than M8 do not have excesses in [4.5] and W2.

To refine our identifications of excesses, we have checked for sources that are redder than the boundaries for [4.5] or W2 in Figure 1 but have data at longer wavelengths that are consistent with a stellar photosphere. All stars of this kind are only slightly above the excess thresholds in [4.5] and W2. Therefore, we indicate that they lack [4.5] and W2 excesses in Table 1. These stars consist of 2MASS J16072682-1855239, 2MASS J16104202-2101319, 2MASS J16133688-2327298, 2MASS J16152024-2333588, 2MASS J16203456-2430205, 2MASS J16204144-2425491, 2MASS J16370753-2432395, Sco PMS 48, HIP 78977, Sco PMS 42b, and HIP 81455. The latter two stars may have small excesses in [24] (Section 3.4), but they lack excess emission in W3. Several stars with excesses in [4.5] or W2 do not have photometry at longer wavelengths, and thus cannot be examined in this way, because they were below the detection limit (W3, W4, [24]) or were not observed ([5.8], [8.0], [24]).

We also have checked for members that have excesses in [4.5] but not W2, or vice versa. Two objects of this kind were discussed earlier in this section in the context of the late-type members. Three additional stars show this discrepancy, consisting of 2MASS J16090075-1908526, 2MASS J16095933-1800090, and RX J1604.3-2130A. As in the earlier cases, variability is the likely cause of the differences between $K_s - [4.5]$ and $K_s - W2$ for these stars given that other bands indicate the presence of disks. For RX J1604.3-2130A, previous IR data have exhibited significant variability as well (Dahm & Carpenter 2009). However, the variability in this star is rather unusual. Its [4.5] – [8.0] color and its spectrum from Dahm & Carpenter (2009) shortward 16 μm are consistent with a stellar photosphere, but the *WISE* bands over this same wavelength range (W1, W2, W3) show excess emission relative to K_s and each other, which may be caused by changes in the structure of the inner disk (Espaillat et al. 2011).

3.2. Excesses in [8.0]

Photometry in [8.0] has been measured for 335 members of Upper Sco. 2MASS J16075850-2039485 is excluded from the diagram of $K_s - [8.0]$ in Figure 1 because its 8 μm flux is uncertain. As done for $K_s - [4.5]$ and $K_s - W2$, we have defined a threshold that varies with spectral type for identifying excesses in $K_s - [8.0]$. It is defined by lines connecting (B0, 0.2), (K0, 0.32), (M0, 0.45), and (M9, 1.01). Excesses from disks are larger at longer wavelengths, resulting in a greater separation between diskless and disk-bearing stars in $K_s - [8.0]$ compared to $K_s - [4.5]$ and $K_s - W2$. In all three of these colors, some of the early-type stars are 0.1–0.2 mag redder than the sequence of the bluest stars. Most of these excesses can be attributed to extinction based on their lack of excesses at longer wavelengths and their red near-

IR colors. However, a few of these moderately red stars may have small amounts of emission from debris disks (Carpenter et al. 2006), even though they appear below our adopted boundaries for excesses in Figure 1. Finally, we have checked for discrepancies between apparent excesses in $K_s - [8.0]$ and data in other bands. 2MASS J16210222-2358395 is slightly above our excess threshold for $K_s - [8.0]$, but $[8.0]$ does not show an excess relative to IRAC and WISE data at shorter wavelengths. Therefore, the excess in $K_s - [8.0]$ may be due to stellar variability between the observations at K_s and the mid-IR bands.

3.3. Excesses in W3

In W3, W4, and [24], some members of Upper Sco are not detected or have large uncertainties in their photometry. For identifying excesses in these bands, we consider only measurements with uncertainties less than 0.25 mag. We also exclude stars that are flagged as extended. These criteria are satisfied in W3 by 658 members. Our adopted threshold for excesses in $K_s - W3$ is shown in Figure 1, which is defined by lines connecting (B0, 0.18), (G8, 0.33), and (M9, 1.52).

For stars that are slightly above the boundary for excesses, we have checked whether excess emission is present in W4 or [24]. HIP 78977 lacks an excess in either band and 2MASS J16233234-2523485 should have little if any excess in W4 based on its non-detection. Therefore, we conclude that these stars probably do not have excesses in W3. Given the limits available at [24] and W4, 2MASS J16181618-2619080, 2MASS J16253672-2224285, 2MASS J16053077-2246200, and 2MASS J16044303-2318258 have colors of $\lesssim 3$ in $K_s - W4$ and $K_s - [24]$, indicating that they could have excess emission at W4 and [24]. Since we cannot rule out the presence of excesses at longer wavelengths, we tentatively classify these stars as having excesses in W3.

Rizzuto et al. (2012) found that HIP 79878 has excess emission in W3, but it is slightly below our threshold for $K_s - W3$. Riaz et al. (2012) reported an excess in W3 for 2MASS J16185037-2424319, but we rejected this measurement as a false detection.

3.4. Excesses in [24] and W4

We discuss the bands [24] and W4 together since they have similar effective wavelengths (23.7 and 22 μm). As with W3, we consider only data with uncertainties less than 0.25 mag and that are not contaminated by extended emission. The resulting sample contains 348 and 260 stars with photometry in [24] and W4, respectively. Data are available in at least one of the two bands for 428 members.

Among the *Spitzer* and *WISE* bands that we are considering, [24] and W4 are the only ones in which debris disks are likely to produce noticeable excess emission (Section 4). Since these excesses can be arbitrarily small, we have defined thresholds in $K_s - [24]$ and $K_s - W4$ that identify the smallest excesses that appear to be significant. The threshold adopted for $K_s - W4$ is higher than that for $K_s - [24]$ since the photometric uncertainties are larger in W4 than in [24], as illustrated by the larger width in the sequence of photospheric colors for $K_s - W4$ in Figure 1. As a result, some stars that show small excesses in $K_s - [24]$ are below the threshold for $K_s - W4$.

The thresholds are defined by (B0, 0.11), (K6, 0.57), and (M9, 1.4) for $K_s - [24]$ and (B0, 0.34) and (M8, 1.15) for $K_s - W4$.

Most of our identifications of excesses in [24] and W4 agree with those from previous studies (Carpenter et al. 2006; Chen et al. 2006, 2011; Cieza et al. 2007; Riaz et al. 2009; Bowler et al. 2011; Rizzuto et al. 2012; Romero et al. 2012), with the following exceptions. Our [24] photometry for HIP 81455 is 0.4 mag brighter than that measured by Chen et al. (2011) with the same data. As a result, we find an excess in this band while Chen et al. (2011) did not. This star is partially resolved from another fainter star at a separation of 8'', which was removed through PSF subtraction prior to our aperture photometry. We speculate that the PSF photometry of Chen et al. (2011) may have been affected by this second star. Chen et al. (2011) found that HIP 78977 has an excess in $K_s - [24]$, but it is slightly below our thresholds for both $K_s - [24]$ and $K_s - W4$. Neither [24] nor W4 show an excess relative to W1, W2, and W3 while excesses do appear in $K_s - W2$ and $K_s - W3$. These discrepant colors are likely caused by variability of the star between the near- and mid-IR observations, and we conclude that it does not have excesses in [24] and W4. The following stars are above our [24] thresholds but slightly below those adopted by Carpenter et al. (2009): HIP 78702, HIP 78099, HIP 76633, HIP 79250, and RX J1602.8-2401B. Rizzuto et al. (2012) used W4 to assess the presence of excess emission for HIP 78265, HIP 80019, HIP 80311, and HIP 82319, but we have rejected these data because they are false detections or too uncertain.

We have identified 22 new candidates in Upper Sco for weak excess emission in [24] or W4, which may indicate the presence of debris disks or evolved transitional disks (see Section 4). Six of these stars were found to lack excesses in previous studies, as described above. The remaining new candidates for weak excesses consist of HD 142506, HIP 80196, 2MASS J16020287-2236139, 2MASS J16050231-1941554, 2MASS J16052459-1954419, 2MASS J16061330-2212537, 2MASS J16080555-2218070, 2MASS J16094098-2217594, 2MASS J16103956-1916524, 2MASS J16104202-2101319, 2MASS J16114612-1907429, 2MASS J16124893-1800525, 2MASS J16230783-2300596, RXJ1614.6-1857, Sco PMS 8b, and Sco PMS 42b. The detection of a W4 excess for HD 142506 is tentative since the photometry may be affected by blending with another star. Similarly, 2MASS J16235695-3312033 is above the threshold for an excess in $K_s - W4$, but it is blended with another star. Because it lacks an excess in the higher-resolution images at [24], we classify this star as lacking an excess in W4.

Unlike the other *Spitzer* bands that we consider, the [24] images did not detect all of the members of Upper Sco that they encompass. Among the members observed in [24], 94 stars were not detected or have errors large enough to be excluded from our analysis. Three of these stars have early spectral types and lack data because they are projected against bright nebulosity or are dominated by extended emission. The remaining 91 objects have M types, most of which are later than M3. A few of these stars have poor constraints on [24] because of bright nebulosity or the PSF of another star, but most have limits of $[24] \sim 10$, indicating that these stars have colors

of $K_s - 24 \lesssim 3.5$. The detection limit from W4 is bright enough ($W4 \sim 8$) that the resulting limits on $K_s - W4$ do not place useful constraints on the presence of disks for most members of Upper Sco that are not detected in this band.

4. CLASSIFICATION OF DISKS

Multiple stages of evolution are usually present among the circumstellar disks in young stellar populations ($\tau \lesssim 10$ Myr). The evolution of a disk is largely characterized by a change in its structure, which is reflected in its IR spectral energy distribution (SED). As a result, one can use multi-band IR data like those we have compiled from *Spitzer* and *WISE* for Upper Sco to estimate the evolutionary stages of disks. In this section, we describe our adopted definitions for these stages and apply them to Upper Sco.

4.1. Terminology

A variety of names and definitions have been devised for the evolutionary stages of disks. We use the ones adopted by Espaillat et al. (2012), which are as follows: A *full disk* is optically thick at IR wavelengths and has not experienced significant clearing as indicated by its SED. A *pre-transitional disk* and a *transitional disk* have gaps and holes in their dust distributions, respectively, that are large enough to noticeably affect their SEDs ($\Delta R_{\text{gap}} > 5$ AU, $R_{\text{hole}} > 1$ AU, Strom et al. 1989; Calvet et al. 2005; Espaillat et al. 2007, 2010). An *evolved disk* is becoming optically thin and does not have a large gap or hole (Hernández et al. 2007). Evolved disks also have been named anemic, thin, weak, and homologously depleted (Lada et al. 2006; Barrado y Navascués et al. 2007; Dahm & Hillenbrand 2007; Currie et al. 2009). Since we are examining a stellar population that includes relatively advanced stages of disk evolution, we also use the terms *evolved transitional disk*, which has optically thin primordial dust and a large inner hole (Luhman et al. 2010), and *debris disk*, which consists of second-generation dust that is generated by collisions among planetesimals (Kenyon & Bromley 2005; Rieke et al. 2005). All of these stages except debris disks are considered *primordial disks*. This definition of a primordial disk differs from the one that we adopted in Luhman et al. (2010), where was equivalent to a full disk as defined here.

4.2. Observational Criteria

To define our observational criteria for the different evolutionary stages of disks, we begin by describing the qualitative features of their SEDs. A full disk produces moderate-to-strong emission throughout the IR regime. Because it has a large inner hole, a transitional disk is faint at shorter IR wavelengths and is much brighter at longer wavelengths. The emission from an evolved disk does not change abruptly with wavelength since it lacks a large hole or gap, and it is very weak since the disk is becoming optically thin. An evolved transitional disk and a debris disk have similar SEDs, showing only weak emission at long IR wavelengths.

To develop quantitative criteria for classifying disks, one approach has been to identify distinct populations in the IR SEDs of young stars and associate them with

different evolutionary stages of disks. Populations of this kind were first found in Taurus, where most stars have mid-IR colors that are either consistent with stellar photospheres, or are much redder. The few sources within the gap between these two groups were described as “in transition” (Strom et al. 1989; Skrutskie et al. 1990). Similar gaps are present in the mid-IR colors of other star-forming regions as well (Luhman et al. 2010, references therein). In some studies, the red edge of the gap in colors like $K_s - [8.0]$ has been adopted as the boundary between full disks and pre-transitional disks on the redward side, and evolved and transitional disks on the blueward side (Hernández et al. 2007; Luhman et al. 2010). This threshold seems reasonable given that it roughly coincides with the colors produced by models of full disks with high degrees of dust settling (Luhman et al. 2010; Espaillat et al. 2012). Distinctive populations of colors and supporting modeling also have been used to guide the identification of debris disks and evolved transitional disks (Carpenter et al. 2009).

A different approach to classifying disks has been employed by Currie & Sicilia-Aguilar (2011). They defined transitional disks to include disks with inner holes or gaps and disks that are optically thin, which correspond to transitional, pre-transitional, and evolved disks in our terminology. To identify disks of this kind, Currie & Sicilia-Aguilar (2011) compared observed SEDs to the SEDs predicted by disk models. When millimeter measurements were available, they also required that a disk have an estimated mass less than $0.001 M_*$ in order for it to be considered optically thin. After applying these procedures, Currie & Sicilia-Aguilar (2011) concluded that some of the disks previously classified as settled, optically thick disks (i.e., redward of the gap in IR colors described above) are instead optically thin, and hence qualify as transitional disks as defined in their study. Because their definition of transitional disks was broader and their classification criteria encompassed redder disks, Currie & Sicilia-Aguilar (2011) found a higher abundance of transitional disks in regions like Taurus than some studies (e.g., Luhman et al. 2010). Of course, a comparison of the abundances of transitional disks, and the resulting evolutionary timescales (Section 5.2), is not meaningful when the adopted definitions of transitional disks differ.

The classification scheme from Currie & Sicilia-Aguilar (2011) has disadvantages. Transitional disks are not defined in the traditional manner (disks with large holes), which can lead to confusion when classifications from different studies are compared. The observational criteria from Currie & Sicilia-Aguilar (2011) rely on theoretical SEDs, which are subject to imperfections in the physical prescriptions of the models and degeneracies among the disk parameters. The predicted SEDs also can vary from one set of adopted models to another. For instance, as indicated above, some objects can be reproduced with either an optically thin disk or a settled optically thick disk, depending on the choice of models (Luhman et al. 2010; Currie & Sicilia-Aguilar 2011; Espaillat et al. 2012). The use of disk mass as a criterion for identifying optically thin disks is also problematic. The requisite millimeter data are unavailable for many members of young clusters and

are incomplete at low disk masses, even in Taurus (Andrews & Williams 2005). Estimates of disk masses and optical depths are sensitive to both the disk model and the opacities that are adopted (Espaillat et al. 2012). In addition, Currie & Sicilia-Aguilar (2011) selected a threshold of $0.001 M_*$ as a lower mass limit for optically thick disks because nearly all optically thick disks in Taurus with millimeter data have masses above this value. However, $0.001 M_*$ is only slightly above the detection limits for the millimeter observations in Taurus ($\gtrsim 0.0005 M_\odot$, Andrews & Williams 2005), and hence does not represent a measurement of the minimum mass of optically thick disks. Deeper millimeter data are needed to reliably determine the distribution of disk masses down to low optical depths.

In a critique of the disk classifications based on colors from Luhman et al. (2010), Currie & Sicilia-Aguilar (2011) noted that UX Tau A has a disk with a large gap (Espaillat et al. 2007) but did not satisfy the color criteria for a transitional disk from Luhman et al. (2010) and instead was classified as a primordial disk (or a full disk with our current terminology). However, this classification was consistent with the definitions adopted by Luhman et al. (2010) in which a disk with a gap was considered pre-transitional and a subset of primordial disks, whereas only disks with large holes were named transitional. Any set of classification criteria will exclude disks with holes or gaps below a certain size, so the absence of disks with gaps like UX Tau A from our definition of transitional disk is not particularly worrisome. We simply use the term “transitional disk” to refer to a different range of structural evolution than Currie & Sicilia-Aguilar (2011).

In summary, we have selected a classification scheme for disks in which the evolutionary stages are defined by distinct structural characteristics (Espaillat et al. 2012). The criteria for identifying members of these classes are based on patterns in the data for disks (e.g., gap in colors) and can be applied to data that are available for large numbers of young stars and brown dwarfs, namely multi-band mid-IR photometry from *Spitzer* and *WISE*.

4.3. Disk Classes in Upper Sco

In Luhman et al. (2010), we used extinction-corrected mid-IR colors to estimate the evolutionary stages of disks in Taurus and other regions. For Upper Sco, we modify this approach by considering instead the color excesses relative to photospheric colors (e.g., $E(K_s - [24])$). We have computed the excess in a given color for each member of Upper Sco by subtracting the color of a stellar photosphere in Upper Sco for the spectral type in question, as determined by a fit to the sequence of diskless stars in Figure 1. Through this process, the colors for all members are corrected for roughly the same level of extinction, which is the average extinction of the diskless members. The resulting excesses for the colors from Figure 1 are presented in Figure 2. The Be stars are omitted since they do not require classification. We plot the excesses based on [4.5] and W2 together because of the similarity of these bands. We do the same for [24] and W4. For each object, we show the data in [4.5] and [24] when available, and otherwise use W2 and W4.

Luhman et al. (2010) used $K_s - [5.8]$, $K_s - [8.0]$, and $K_s - [24]$ for their disk classifications. Since relatively

few members of Upper Sco have been observed in [5.8], we begin our classifications with the other two colors (and $K_s - W4$). In Figure 2, we show our adopted thresholds in $E(K_s - [8.0])$ and $E(K_s - [24])/W4$ for distinguishing between full disks and later evolutionary stages. These thresholds approximate those applied to $K_s - [8.0]$ and $K_s - [24]$ by Luhman et al. (2010). We have used the objects classified in this way to reveal the boundary between full disks and later stages in $E(K_s - W3)$ vs. $E(K_s - [24])/W4$, and we have used this boundary to classify stars that lack data in [8.0]. To classify the disks bluer than full disks, we apply the following criteria, which are similar to those from Carpenter et al. (2009) and Luhman et al. (2010): transitional disks have $E(K_s - [24])/W4 > 3.2$; evolved disks have $E(K_s - [24])/W4 < 3.2$, $E(K_s - [8.0]) > 0.3$, and $E(K_s - W3) > 0.5$; debris disks and evolved transitional disks have $E(K_s - [24])/W4 < 3.2$, $E(K_s - [8.0]) < 0.3$, and $E(K_s - W3) < 0.5$. Measurements of gas content are necessary for distinguishing between the latter two classes of disks since they exhibit similar mid-IR SEDs (Carpenter et al. 2009), but such data are unavailable for most disks in Upper Sco. For the early-type stars, the high abundance of these debris/evolved transitional candidates relative to full disks indicates that most are probably debris disks since evolved transitional disks are expected to be short-lived (Section 5.2). Two exceptions to the above criteria are HIP 79288 and HIP 79977. Both stars are redder than our thresholds for debris/evolved transitional disks, but we classify them as such based on previous studies (Sylvester & Mannings 2000; Honda et al. 2004; Smith et al. 2008; Chen et al. 2006, 2011).

We have attempted to classify the disks that lack photometry in [24] or W4, and hence do not appear in Figure 2. For the disks of this kind that are detected in W3, the excesses in this band are small enough to indicate that they are evolved or transitional. Some of those disks are probably evolved rather than transitional based on the available constraints on $E(K_s - [24])/W4$. Two of the disks without W3, W4, or [24] have data in [8.0], both of which are full disks according to their values of $E(K_s - [8.0])$. The remaining disks that lack data in [24] or W4 are detected only at $\lambda < 5 \mu\text{m}$, most of which are later than M6. We classify them as full disks for the purposes of this work, although some could be evolved disks.

In Table 1, we present our disk classifications for all members of Upper Sco that show mid-IR excess emission. Through our classifications, we arrive at 135 full disks, 28 evolved disks, 6 transitional disks, three disks that are evolved or transitional, and 63 debris/evolved transitional disks. Previous mid-IR studies have already identified many of these full disks (Carpenter et al. 2006; Scholz et al. 2007; Riaz et al. 2012), evolved and transitional disks (Riaz et al. 2009; Dahm & Carpenter 2009; Dahm 2010; Luhman et al. 2010), and debris/evolved transitional disks (Cieza et al. 2007; Carpenter et al. 2009; Chen et al. 2006, 2011; Romero et al. 2012). Our new candidates for transitional disks consist of 2MASS J16082733-2217292, 2MASS J16101888-2502325, and 2MASS J16151239-2420091. It is likely that a number of full disks have inner holes that are too small to be classified as transitional using our criteria, such as 2MASS

J16081566-2222199, which has strong excesses in W3 and W4 but no excess in W2 (see upper panel of Figure 2). Most of the candidates for evolved disks are newly identified as such in this work. In Section 3.4, we listed our new candidates for debris/evolved transitional disks and a few stars in this category that we classify differently than other studies. We note that HIP 81474 has been frequently treated as a Herbig Ae/Be star, but it lacks a clear detection of line emission (Hernández et al. 2005). Therefore, it is classified as debris/evolved transitional in this work.

5. STATISTICAL PROPERTIES OF EXCESSES

5.1. *Excess Fractions*

The distribution of disk excesses as a function of parameters like wavelength, spectral type, cluster age, excess size, and disk class can provide insight into the evolution of disks. To characterize the distribution of excesses in Upper Sco, we begin by considering the fraction of members that exhibit excesses. In Table 2 and Figure 3, we present the excess fraction as a function of spectral type for [4.5]/W2, [8.0], W3, and [24]/W4. To examine the evolution of primordial and debris disks separately, one excess fraction is computed for full, transitional, and evolved disks, and another is computed for debris and evolved transitional disks. The latter disks do contain primordial dust, but they cannot be distinguished from debris disks with available data, as discussed in the previous section.

The images in W3, W4, and [24] were not sufficiently sensitive to detect all known members of Upper Sco. The members that were too faint to be detected tend to have later spectral types or smaller excesses. As a result, we cannot compute meaningful excess fractions in these bands at the latest types. Therefore, the excess fractions for W3 and [24]/W4 in Figure 3 are shown only for spectral types in which nearly all of the known members are detected. For the joint [24]/W4 excess fraction, we adopt the [24] data when available, which have a high level of completeness down to a spectral type of M4. Among [24] non-detections earlier than M4, six stars were not subject to extended emission or blending with other stars, and hence have useful limits on their photometry. The resulting constraints on $K_s - [24]$ indicate that these six stars have little, if any, excess emission, so we include them as non-excess stars in the [24]/W4 fraction. Among stars that were not observed at [24], the W4 images detected all but three stars earlier than M0. Therefore, we use the W4 data of members not observed at [24] and earlier than M0 in the [24]/W4 fraction. The three stars earlier than M0 with non-detections in W4 have sufficient constraints on this band to indicate that excesses are probably not present, so we count them as non-excess stars. It is unnecessary to impose such restrictions on the spectral types included in the excess fractions at [4.5], W2, and [8.0] since all known members were detected in these bands as long as they were observed (by IRAC) and not blended with another star. The Be stars are excluded from these excess fractions.

We first discuss the excess fractions for the full, transitional, and evolved disks (i.e., all primordial disks except for evolved transitional disks). For these disks, the excess fractions are very low at a roughly uniform level as a

function of spectral type for B through G types, and then increase with later types from K through M. This trend was discovered by Carpenter et al. (2006), supported by additional data from Scholz et al. (2007) for late-M members, and now is reinforced further with better number statistics. All of the bands in Figure 3 exhibit a similar dependence on spectral type, except that the excess fractions are slightly higher at longer wavelengths due to the presence of a small number of transitional disks. As discussed by Carpenter et al. (2006), these data indicate that disk lifetimes are longer for stars at lower masses, providing more time for planet formation. We note that the excess fraction in [4.5]/W2 for the last bin in Figure 3 at M8–L2 ($\sim 0.01 M_\odot$) is uncertain because of the small number of objects and the rapidly changing photospheric colors, which makes it difficult to reliably identify excesses. In addition, since excesses in [4.5] are smaller at later types (Luhman et al. 2010), the excess fraction in this band may significantly underestimate the disk fraction. Longer wavelengths are needed for more robust detections of disk excesses for brown dwarfs, but the members at M8–L2 were too faint for W3 and W4 photometry and were not observed at [5.8] and [8.0]. The disk fractions based on the data in Figure 3 are compared to similar measurements in younger clusters by Luhman (2012).

We now consider the excess fractions for the debris and evolved transitional disks. As mentioned earlier, we cannot distinguish between these two types of disks with the mid-IR data, but most of the candidates at earlier spectral types are probably debris disks. It is unclear which class of disk dominates at later types. In Figure 3, the excess fraction for this sample increases rapidly with longer wavelengths. Excesses in [4.5]/W2 are present for only a few stars, which may be some of the youngest debris disks in the association (Sylvester & Mannings 2000; Honda et al. 2004; Smith et al. 2008; Chen et al. 2006, 2011). The [24]/W4 fraction is highest for A stars (~ 0.4), drops sharply for B stars (< 0.07), and decreases more gradually with later types, reaching 0.1–0.2 for G, K, and M stars. These trends are consistent with those previously found in smaller samples of [24] data in Upper Sco by Carpenter et al. (2009) and Chen et al. (2011). Those studies investigated various aspects of their [24] data, and their results apply to our new measurements as well. For instance, Carpenter et al. (2009) found that the rapid decrease in [24] fraction from A to B stars is expected because of increased ejection of dust grains by radiation pressure (see also Kenyon & Bromley 2008). The [24]/W4 excess fractions at later spectral types are more difficult to interpret since they contain an unknown contribution from evolved transitional disks. In addition, many debris disks around late-type stars may be too cool to produce noticeable excesses in these bands. Carpenter et al. (2009) and Chen et al. (2011) also examined the evolution of debris disks by comparing the [24] excess fractions among Upper Sco and other associations and clusters across a range of ages (see also Siegler et al. 2007; Currie et al. 2008; Gaspar et al. 2009). Our data have improved the statistical constraints on excess fractions and sizes in Upper Sco, particularly at M types, but an analysis like that from Carpenter et al. (2009) and Chen et al. (2011) for M stars is not possible because sufficiently complete samples of [24] data are

available for only a few regions.

5.2. Sizes of Excesses at $[24]$ and $W4$

The mid-IR colors of the members of a given star-forming region typically exhibit a gap between diskless stars and the bulk of the disk-bearing stars (see Section 4.2). This trough in the distribution of excess sizes has been previously interpreted as evidence that once a disk has begun to clear to a certain degree, the remainder of the dust in the inner disk clears rapidly (Skrutskie et al. 1990). In this section, we examine the constraints on the clearing timescale that are provided by the distribution of excesses in Upper Sco.

Because the contrast between a stellar photosphere and circumstellar disk increases at longer IR wavelengths, $[24]$ and $W4$ offer the largest dynamic range in the sizes of excesses among the photometric bands that we have compiled for Upper Sco. Given that the $[24]$ observations are more sensitive than those at $W4$, we choose the former for constructing the distribution of excesses. To characterize how this distribution changes with cluster age, we compare the data for Upper Sco to measurements of $[24]$ in Taurus (Luhman et al. 2010). Upper Sco and Taurus are the best available regions for such a comparison since they roughly bracket the ages of primordial disks (~ 1 and 10 Myr), contain two of the richest and nearest samples of young stars, and have been thoroughly observed by *Spitzer*. In particular, few other regions have $[24]$ measurements that reach the stellar photospheres of low-mass stars, which is essential for fully sampling excesses across all sizes. Since very few primordial disks are present among the early-type stars in Upper Sco, we exclude stars earlier than K0 from the distributions of $K_s - [24]$ excesses for Upper Sco and Taurus. We also omit stars later than M5 since most of the diskless stars at these types are below the detection limits of the $[24]$ images. Roughly a dozen stars in each region at K5–M5 are not detected in $[24]$ and could have small excesses based on the limits on $K_s - [24]$. As a result, the distributions of excesses that we construct are biased slightly against small excesses.

The distributions of $E(K_s - [24])$ for K0–M5 members of Taurus and Upper Sco are presented in Figure 4, excluding protostellar sources. The two distributions exhibit similar troughs at $E(K_s - [24]) \sim 0.5$ – 3 . Most observations of other young clusters at $[24]$ are less complete at low excesses or consider smaller numbers of stars, but they are generally consistent with gaps of this kind (Luhman et al. 2010). Meanwhile, among stars redward of the trough ($E(K_s - [24]) > 3$), the average color is bluer in Upper Sco than in Taurus. These characteristics can be explained in the following manner. The youngest systems have highly flared disks, and hence the largest IR excesses. As they evolve (e.g., growth of grains, accretion onto the star), disks become more settled and produce smaller excesses. After disks have become highly settled and have reached a certain level of initial clearing (corresponding to $E(K_s - [24]) \sim 3$), they quickly clear their remaining inner disks, resulting in a scarcity of disks with small excesses. Because star formation is ongoing in Taurus but has ceased in Upper Sco, the distribution of excesses in the former is more heavily weighted to younger and redder disks. In other words, the youngest disks in Upper Sco have already evolved

substantially, explaining its paucity of very red disks relative to Taurus. Because the evolutionary stages of disks are not sampled in the same way by the differing star formation histories of Taurus and Upper Sco, a comparison of the $N(\text{evolved} + \text{transitional})/N(\text{full})$ does not indicate the relative timescales of clearing between the two populations (Luhman et al. 2010). Instead, one must compare the ratio of the number of evolved and transitional disks to the number of sources slightly redward of the trough, i.e., the shape of the distribution of excesses at $E(K_s - [24]) \lesssim 3.5$. This property is not tightly constrained in either region because of the small numbers of stars involved, but Taurus and Upper Sco do not show any obvious differences. Thus, there is no evidence to indicate that the clearing timescale changes from the age of Taurus to the age of Upper Sco (~ 1 – 10 Myr). The data in Figure 4 do reveal a higher abundance of candidates for evolved transitional disks or debris disks in Upper Sco. If the lifetime of the evolved transitional stage is similar to that of the transitional and evolved stages, then most of these candidates in Upper Sco are probably debris disks. It is expected that Upper Sco would contain more debris disks than Taurus given their relative ages.

As discussed in Section 4.2, the definition of transitional disks adopted by Currie & Sicilia-Aguilar (2011) encompasses some of the objects redward of the gap in the mid-IR colors in regions like Taurus and Upper Sco. As a result, they have derived higher abundances of transitional disks in young clusters, and hence a longer timescale for inner disk clearing, than found here and in other studies that use a more restrictive definition for transitional disks (Hernández et al. 2007; Luhman et al. 2010). Of course, it is not meaningful to compare abundances of transitional disks and the resulting timescales among studies that do not define this evolutionary stage in the same manner. We contend that the clearing timescales from Currie & Sicilia-Aguilar (2011) are less useful and practical since they are based on a definition of transitional disks that is subject to uncertainties and degeneracies in model SEDs and that does not rely on distinct observational signatures (i.e., gap in colors).

Currie et al. (2009) suggested that the gap in mid-IR colors in Taurus is not evidence of a short lifetime for the evolutionary stage of disks within this gap, contrary to the original interpretation (Skrutskie et al. 1990). Instead, they argued that the gap is present because few members of Taurus are old enough to have reached that stage, and that the diskless stars in Taurus have lost their disks due to binary companions rather than advanced age. In Luhman et al. (2010), we noted that a rather large fraction of the Taurus population is diskless (40% among non-protostars) and that these stars are older than disk-bearing members, on average, based on their wider spatial distribution, demonstrating that a significant number of stars in Taurus have aged sufficiently to fully clear their disks, and hence pass through the evolved and transitional stages. Currie & Sicilia-Aguilar (2011) reiterated the same points from their previous study, but also conceded that many of the diskless stars in Taurus may indeed be older than their counterparts with disks. Here, we once again contend that if a significant number of stars have aged sufficiently to have fully cleared their disks, then the evolved and transitional stages should be fully sampled as well, and therefore their scarcity demon-

strates that they are short-lived relative to full disks. This conclusion is supported by the fact that older regions like Upper Sco exhibit the same gap in their colors (Figure 4; Luhman et al. 2010, references therein).

6. CONCLUSIONS

We have performed a census of the circumstellar disk population of the Upper Sco association ($\tau \sim 11$ Myr) using mid-IR images obtained with the *Spitzer Space Telescope* and *WISE*. The results of this study are summarized as follows:

1. We have analyzed all images of known members of Upper Sco at 3.6, 4.5, 5.8, 8.0, and 24 μm that have been collected by *Spitzer* to date. Among the 863 known members, 484 have been observed in at least one of these bands. We have presented a catalog of photometry and non-detections for these objects.
2. We have compiled all photometry at 3.4, 4.6, 12, and 22 μm (W1–W4) for members of Upper Sco from the *WISE* mission, thoroughly vetting these data for false detections, blends with neighboring stars, and extended emission. All resolved, unblended members were detected by *WISE* in at least 3.4 and 4.6 μm .
3. We have used colors computed between K_s and six of the *Spitzer* and *WISE* bands to identify the members that exhibit excess emission from circumstellar disks. We have estimated the evolutionary stages of the detected disks using the sizes of the excesses among these bands. These stages are defined based on distinct structural characteristics that are apparent in the SEDs (Espaillat et al. 2012, references therein), and they consist of the following: optically thick disks without large holes or gaps (*full*), optically thick disks with large holes (*transitional*), optically thin disks without large holes or gaps (*evolved*), optically thin disks with large holes (*evolved transitional*), and disks of second-generation dust (*debris*). Through these classifications, we have found ~ 50 new candidates for transitional, evolved, and debris disks.

4. Based on our census of disks, the fraction of Upper Sco members with inner primordial disks is $\lesssim 10\%$ for B–G stars ($M > 1.2 M_\odot$) and increases with later types, reaching $\sim 25\%$ at M5–L0 ($M \sim 0.01\text{--}0.2 M_\odot$). This trend was first observed by Carpenter et al. (2006), and is now reinforced with a sample that is larger and reaches lower stellar masses. The combination of these data and the latest age estimate for Upper Sco ($\tau \sim 11$ Myr, Pecaute et al. 2012) indicate that a significant fraction of primordial disks around low-mass stars survive for at least ~ 10 Myr.

5. K0–M5 members of Upper Sco show a dearth of disks with small excesses (transitional and evolved disks). When the differences in star formation histories of Upper Sco and Taurus ($\tau \sim 1$ Myr) are taken into account, the distributions of excesses for both regions indicate a timescale for inner disk clearing that is much shorter than the typical lifetime of primordial disks.

We thank Catherine Espaillat, Nuria Calvet, and Eric Feigelson for comments on the manuscript. K. L. was supported by grants AST-0544588 and NNX12AI58G from the National Science Foundation and the NASA Astrophysics Data Analysis Program, respectively, and E. M. was supported by grant AST-1008908 from the National Science Foundation. This work makes use of data from the *Spitzer Space Telescope*, 2MASS, *WISE*, and the Infrared Processing and Analysis Center (IPAC) Infrared Science Archive (IRSA). *Spitzer* and IRSA are operated by the Jet Propulsion Laboratory (JPL) and the California Institute of Technology (Caltech) under contract with NASA. *WISE* is a joint project of the University of California, Los Angeles, and JPL/Caltech, funded by NASA. 2MASS is a joint project of the University of Massachusetts and the IPAC/Caltech, funded by NASA and the NSF. The Center for Exoplanets and Habitable Worlds is supported by the Pennsylvania State University, the Eberly College of Science, and the Pennsylvania Space Grant Consortium.

REFERENCES

- Allers, K. N., Jaffe, D. T., Luhman, K. L., et al. 2007, *ApJ*, 657, 511
- Andrews, S. M., & Williams, J. P. 2005, *ApJ*, 631, 1134
- Ardila, D., Martín, E. L., & Basri, G. 2000, *AJ*, 120, 479
- Baraffe, I., Chabrier, G., Allard, F., & Hauschildt, P. H. 1998, *A&A*, 337, 403
- Barrado y Navascués, D., Stauffer, J. R., Morales-Calderón, M., et al. 2007, *ApJ*, 664, 481
- Béjar, V. J. S., Zapatero Osorio, M. R., Pérez-Garrido, A., et al. 2008, *ApJ*, 673, L185
- Billier, B., Allers, K., Liu, M., Close, L. M., & Dupey, T. 2011, *AJ*, 730, 39
- Bowler, B. P., Liu, M. C., Kraus, A. L., Mann, A. W., & Ireland, M. J. 2011, *ApJ*, 743, 148
- Calvet, N., D'Alessio, P., Watson, D. M., et al. 2005, *ApJ*, 630, L185
- Carpenter, J. M., Mamajek, E. E., Hillenbrand, L. A., & Meyer, M. R. 2006, *ApJ*, 651, L49
- Carpenter, J. M., Bouwman, J., Silverstone, M. D., et al. 2008, *ApJS*, 179, 423
- Carpenter, J. M., Mamajek, E. E., Hillenbrand, L. A., & Meyer, M. R. 2009, *ApJ*, 705, 1646
- Casali, M., Adamson, A., Alves de Oliveira, C., et al. 2007, *A&A*, 467, 777
- Chabrier, G., Baraffe, I., Allard, F., & Hauschildt, P. 2000, *ApJ*, 542, 464
- Chen, C. H., Jura, M., Gordon, K. D., & Blaylock, M. 2005, *ApJ*, 623, 493
- Chen, C. H., Mamajek, E. E., Bitner, M. A., et al. 2011, *ApJ*, 738, 122
- Chen, C. H., Sargent, B. A., Bohac, C., et al. 2006, *ApJS*, 166, 351
- Cieza, L., Padgett, D. L., Stapelfeldt, K. R., et al. 2007, *ApJ*, 667, 308
- Cieza, L. A., Schreiber, M. R., Romero, G. A., et al. 2010, *ApJ*, 712, 925
- Close, L. M., Zuckerman, B., Song, I., et al. 2007, *ApJ*, 660, 1492
- Corbally, C. J. 1984, *ApJS*, 55, 657
- Coté, J., & van Kerkwijk, M. H. 1993, *A&A*, 274, 870
- Cowley, A., Cowley, C., Jaschek, M., & Jaschek, C. 1969, *AJ*, 74, 375

- Crampton, D. 1968, *AJ*, 73, 338
- Currie, T., Plavchan, P., & Kenyon, S. J. 2008, *ApJ*, 688, 597
- Currie, T., Lada, C. J., Plavchan, P., Robitaille, T. P., Irwin, J., & Kenyon, S. J. 2009, *ApJ*, 698, 1
- Currie, T., & Sicilia-Aguilar, A. 2011, *ApJ*, 732, 24
- Cutri, R. M., Wright, E. L., Conrow, T., et al. 2012, Explanatory Supplement to the WISE All-Sky Data Release Products
- Dahm, S. E. 2010, *AJ*, 140, 1444
- Dahm, S. E., & Hillenbrand, L. A. 2007, *AJ*, 133, 2072
- Dahm, S. E., & Carpenter, J. M. 2009, *AJ*, 137, 4024
- Dotter, A., Chaboyer, B., Jevremović, D., et al. 2008, *ApJS*, 178, 89
- de Geus, E. J., de Zeeuw, P. T., & Lub, J. 1989, *A&A*, 216, 44
- Eisner, J. A., Hillenbrand, L. A., White, R. J., Akeson, R. L., & Sargent, A. I. *ApJ*, 623, 952
- Espaillet, C., Calvet, N., D'Alessio, P., et al. 2007, *ApJ*, 670, L135
- Espaillet, C., D'Alessio, P., Hernández, J., et al. 2010, *ApJ*, 717, 441
- Espaillet, C., Furlan, E., D'Alessio, P., et al. 2011, *ApJ*, 728, 49
- Espaillet, C., Ingleby, L., Hernández, J., et al. 2012, *ApJ*, 747, 103
- Evans, N. J., II, Dunham, M. M., Jørgensen, J. K., et al. 2009, *ApJS*, 181, 321
- Fazio, G. G., Hora, J. L., Allen, L. E., et al. 2004, *ApJS*, 154, 10
- Garrison, R. F. 1967, *ApJ*, 147, 1003
- Gaspar, A., Rieke, G. H., Su, K. Y. L., et al. 2009, *ApJ*, 697, 1578
- Gizis, J. E. 2002, *ApJ*, 575, 484
- Gutermuth, R. A., Megeath, S. T., Myers, P. C., et al. 2009, *ApJS*, 184, 18
- Hambly, N. C., Collins, R. S., Cross, N. J. G., et al. 2008, *MNRAS*, 384, 637
- Herczeg, G. J., Cruz, K. L., & Hillenbrand, L. A. 2009, *ApJ*, 696, 1589
- Hernández, J., Calvet, N., Hartmann, L., et al. 2005, *AJ*, 129, 856
- Hernández, J., Hartmann, L., Megeath, T., et al. 2007, *ApJ*, 662, 1067
- Hewett, P. C., Warren S. J., Leggett S. K., & Hodgkin S. L., 2006, *MNRAS*, 367, 545
- Hodgkin, S. T., Irwin, M. J., Hewett, P. C., & Warren, S. J. 2009, *MNRAS*, 394, 675
- Honda, M., Katata, H., Okamoto, Y. K., et al. 2004, *ApJ*, 610, L49
- Houk, N. 1982, Catalogue of Two-dimensional Spectral Types for the HD Stars. Vol. 3, (Ann Arbor: Univ. Mich.)
- Houk, N., & Smith-Moore, M. 1988, Michigan Catalogue of Two-dimensional Spectral Types for the HD Stars. Vol. 4, (Ann Arbor: Univ. Mich.)
- Ireland, M. J., Kraus, A., Martinache, F., Law, N., & Hillenbrand, L. A. 2011, *ApJ*, 726, 113
- Jaschek, C., Jaschek, M., & Kucwicz, B. 1964, *Z. Astrophys.*, 59, 108
- Jayawardhana, R., & Ivanov, V. D. 2006, *Science*, 313, 1279
- Kenyon, S. J., & Bromley, B. C. 2005, *ApJ*, 130, 269
- Kenyon, S. J., & Bromley, B. C. 2008, *ApJS*, 179, 451
- Kimeswenger, S., Lederle, C., Richichi, A., et al. 2004, *A&A*, 413, 1037
- Kraus, A. L., & Hillenbrand, L. A. 2007, *ApJ*, 664, 1167
- Kraus, A. L., & Hillenbrand, L. A. 2009, *ApJ*, 703, 1511
- Kraus, A. L., White, R. J., & Hillenbrand, L. A. 2005, *ApJ*, 633, 452
- Kunkel, M. 1999, Ph.D. thesis, Julius-Maximilians-Univ., Würzburg
- Lada, C. J., Muench, A. A., Luhman, K. L., et al. 2006, *AJ*, 131, 1574
- Lafrenière, D., Jayawardhana, R., Janson, M., et al. 2011, *ApJ*, 730, 42
- Lafrenière, D., Jayawardhana, R., & van Kerkwijk, M. H. 2008, *ApJ*, 689, L153
- Lawrence, A., Warren, S. J., Almaini, O., et al. 2007, *MNRAS*, 379, 1599
- Lodieu, N., Dobbie, P. D., & Hambly, N. C. 2011, *A&A*, 527, A24
- Lodieu, N., Hambly, N. C., & Jameson, R. F. 2006, *MNRAS*, 373, 95
- Lodieu, N., Hambly, N. C., Jameson, R. F., & Hodgkin, S. T. 2008, *MNRAS*, 383, 1385
- Lodieu, N., Hambly, N. C., Jameson, R. F., et al. 2007, *MNRAS*, 374, 372
- Luhman, K. L. 2005, *ApJ*, 633, L41
- Luhman, K. L. 2012, *ARA&A*, in press
- Luhman, K. L., Allen, L. E., Allen, P. R., et al. 2008, *ApJ*, 675, 1375
- Luhman, K. L., Allers, K. N., Jaffe, D. T., et al. 2007, *ApJ*, 659, 1629
- Luhman, K. L., Allen, P. R., Espaillat, C., Hartmann, L., & Calvet, N. 2010, *ApJS*, 186, 111
- Lutz, T. E., & Lutz, J. H. 1977, *AJ*, 82, 431
- Martín, E. L. 1998, *AJ*, 115, 351
- Martín, E. L., Delfosse, X., & Guieu, S. 2004, *AJ*, 127, 449
- Martín, E. L., Montmerle, T., Gregorio-Hetem, J., & Casanova, S. 1998, *MNRAS*, 300, 733
- Martín, E. L., Phan-Bao, N., Bessell, M., et al. 2010, *A&A*, 517, A53
- Merrill, P. W., & Burwell, C. G. 1933, *ApJ*, 78, 87
- Padgett, D. L., Cieza, L., Stapelfeldt, K. R., et al. 2006, *ApJ*, 645, 1283
- Palla, F., & Stahler, S. W. 1999, *ApJ*, 525, 772
- Pecaut M. J., Mamajek E. E., & Bubar E. J. 2012, *ApJ*, 746, 154
- Prato, L. 2007, *ApJ*, 657, 338
- Prato, L., Greene, T. P., & Simon, M. 2003, *ApJ*, 584, 853
- Preibisch, T., Brown, A. G. A., Bridges, T. Guenther, E., & Zinnecker, H. 2002, *AJ*, 124, 404
- Preibisch, T., Guenther, E., & Zinnecker, H. 2001, *AJ*, 121, 1040
- Preibisch, T., Guenther, E., Zinnecker, H., et al. 1998, *A&A*, 333, 619
- Preibisch, T., & Mamajek, E. 2008, in *Handbook of Star Forming Regions*, Vol. 2, The Southern Sky, ASP Monograph Series 5, ed. B. Reipurth (San Francisco, CA: ASP), 235
- Rebull, L. M., Padgett, D. L., McCabe, C.-E., et al. 2010, *ApJS*, 186, 259
- Riaz, B., Gizis, J. E., & Harvin, J. 2006, *AJ*, 132, 866
- Riaz, B., Lodieu, N., Gizis, J. E. 2009, *ApJ*, 705, 1173
- Riaz, B., Lodieu, N., Goodwin, S., Stamatellos, D., & Thompson, M. 2012, *MNRAS*, 420, 2497
- Rieke, G. H., Young, E. T., Engelbracht, C. W., et al. 2004, *ApJS*, 154, 25
- Rieke, G. H., Su, K. Y. L., Stansberry, J. A., et al. 2005, *ApJ*, 620, 1010
- Rizzuto, A. C., Ireland, M. J., & Zucker, D. B. 2012, *MNRAS*, 421, L97
- Romero, G. A., Schreiber, M. R., Cieza, L. A., et al. 2012, *ApJ*, 749, 79
- Scholz, A., Jayawardhana, R., Wood, K., et al. 2007, *ApJ*, 660, 1517
- Sicilia-Aguilar, A., Hartmann, L., Calvet, N., et al. 2006, *ApJ*, 638, 897
- Siegler, N., Muzerolle, J., Young, E. T., et al. 2007, *ApJ*, 654, 580
- Shkolnik, E., Liu, M. C., & Reid, I. N. 2009, *ApJ*, 699, 649
- Skrutskie, M., Cutri, R. M., Stiening, R., et al. 2006, *AJ*, 131, 1163
- Skrutskie, M. F., Dutkevitch, D., Strom, S. E., Edwards, S., Strom, K. M., & Shure, M. A. 1990, *AJ*, 99, 1187
- Slesnick, C. L., Carpenter, J. M., & Hillenbrand, L. A. 2006, *AJ*, 131, 3016
- Slesnick, C. L., Hillenbrand, L. A., & Carpenter, J. M., 2008, *ApJ*, 688, 377
- Smith, R., Wyatt, M. C., & Dent, W. R. F. 2008, *A&A*, 485, 897
- Song, I., Zuckerman, B., & Bessell, M. S. 2012, *AJ*, 144, 8
- Strom, K. M., Strom, S. E., Edwards, S., Cabrit, S., & Skrutskie, M. F. 1989, *AJ*, 97, 1451
- Sylvester, R. J., & Mannings, V. 2000, *MNRAS*, 313, 73
- The, P. S., Wesselius, P. R., & Janssen, I. M. H. H. 1986, *A&AS*, 66, 63
- Torres, C. A. O., Quast, G. R., Da Silva, L., et al. 2006, *A&A*, 460, 695
- van Leeuwen, F. 2007, *A&A*, 474, 653
- Walter, F. M., Vrba, F. J., Mathieu, R. D., Brown, A., & Myers, P. C. 1994, *AJ*, 107, 692
- Werner, M. W., Roellig, T. L., Low, F. J., et al. 2004, *ApJS*, 154, 1
- Wright, E. L., Eisenhardt, P. R. M., Mainzer, A. K., et al. 2010, *AJ*, 140, 1868

TABLE 1
DATA FOR MEMBERS OF UPPER SCO

Column Label	Description
Name	Source name ^a
OtherNames	Other source names ^b
SpType	Spectral type
r_SpType	Spectral type reference ^c
Adopt	Adopted spectral type
3.6mag	<i>Spitzer</i> [3.6] band magnitude
e_3.6mag	Error in [3.6] band magnitude
f_3.6mag	Flag on [3.6] band magnitude ^d
4.5mag	<i>Spitzer</i> [4.5] band magnitude
e_4.5mag	Error in [4.5] band magnitude
f_4.5mag	Flag on [4.5] band magnitude ^d
5.8mag	<i>Spitzer</i> [5.8] band magnitude
e_5.8mag	Error in [5.8] band magnitude
f_5.8mag	Flag on [5.8] band magnitude ^d
8.0mag	<i>Spitzer</i> [8.0] band magnitude
e_8.0mag	Error in [8.0] band magnitude
f_8.0mag	Flag on [8.0] band magnitude ^d
24mag	<i>Spitzer</i> [24] band magnitude
e_24mag	Error in [24] band magnitude
f_24mag	Flag on [24] band magnitude ^d
W1mag	<i>WISE</i> W1 band magnitude ^e
e_W1mag	Error in W1 band magnitude
f_W1mag	Flag on W1 band magnitude ^d
W2mag	<i>WISE</i> W2 band magnitude ^e
e_W2mag	Error in W2 band magnitude
f_W2mag	Flag on W2 band magnitude ^d
W3mag	<i>WISE</i> W3 band magnitude ^e
e_W3mag	Error in W3 band magnitude
f_W3mag	Flag on W3 band magnitude ^d
W4mag	<i>WISE</i> W4 band magnitude ^e
e_W4mag	Error in W4 band magnitude
f_W4mag	Flag on W4 band magnitude ^d
Exc4.5	Excess present in [4.5]?
Exc8.0	Excess present in [8.0]?
Exc24	Excess present in [24]?
ExcW2	Excess present in W2?
ExcW3	Excess present in W3?
ExcW4	Excess present in W4?
DiskType	Disk type

NOTE. — The table is available in a machine-readable format.

^a Coordinate-based identifications from the 2MASS Point Source Catalog when available. Otherwise, identifications from Allers et al. (2007) and Lodieu et al. (2007) are listed.

^b Designations from the Hipparcos Catalog (van Leeuwen 2007) and the Henry Draper Catalog and other frequently used names.

^c (1) Houk & Smith-Moore (1988); (2) K. Luhman, in preparation; (3) Kunkel (1999); (4) Preibisch et al. (1998); (5) Torres et al. (2006); (6) Lodieu et al. (2006); (7) Lodieu et al. (2008); (8) Houk (1982); (9) Pecaut et al. (2012); (10) Corbally (1984); (11) Shkolnik et al. (2009); (12) Walter et al. (1994); (13) Martín et al. (2010); (14) Preibisch et al. (2002); (15) Kraus & Hillenbrand (2009); (16) Martín et al. (2004); (17) Slesnick et al. (2008); (18) Ardila et al. (2000); (19) Slesnick et al. (2006); (20) Riaz et al. (2006); (21) Herczeg et al. (2009); (22) Preibisch et al. (2001); (23) Bejar et al. (2008); (24) Kraus & Hillenbrand (2007); (25) Lodieu et al. (2011); (26) Biller et al. (2011); (27) Prato et al. (2003); (28) Eisner et al. (2005); (29) Gizis (2002); (30) Prato (2007); (31) Martín et al. (1998); (32) Martín (1998); (33) Cowley et al. (1969); (34) Luhman (2005); (35) Lutz & Lutz (1977); (36) Bowler et. (2011); (37) Romero et al. (2012); (38) Jayawardhana & Ivanov (2006); (39) Close et al. (2007); (40) Luhman et al. (2007); (41) E. Mamajek, unpublished; (42) Garrison (1967); (43) Hernández et al. (2005).

^d nodet = non-detection; sat = saturated; out = outside of the camera's field of view; bl = photometry may be affected by blending with a nearby star; ext = photometry is known or suspected to be contaminated by extended emission (no data given when extended emission dominates); bin = includes an unresolved binary companion; unres = too close to a brighter star to be detected; false = detection from *WISE* catalog that appears false or unreliable based on visual inspection; err = W2 magnitudes brighter than ~6 mag are erroneous.

^e W1 and W2 are from the All-Sky Source Catalog and W3 and W4 are from the Preliminary Release Source Catalog.

TABLE 2
EXCESS FRACTIONS IN UPPER SCO

Spectral Type	Mass ^a (M_{\odot})	[4.5]/W2	[8.0]	W3	[24]/W4
Full, Transitional, and Evolved Disks					
B0–B8	2.8–18	0/25 = < 0.07	0/22 = < 0.08	0/25 = < 0.07	0/26 = < 0.07
B8–A6	1.8–2.8	0/45 = < 0.04	0/40 = < 0.04	1/46 = $0.02^{+0.05}_{-0.01}$	1/45 = $0.02^{+0.05}_{-0.01}$
A6–F4	1.5–1.8	0/20 = < 0.09	0/12 = < 0.13	1/21 = $0.05^{+0.09}_{-0.02}$	1/21 = $0.05^{+0.09}_{-0.02}$
F4–G2	1.4–1.5	0/18 = < 0.09	0/9 = < 0.17	0/18 = < 0.09	0/17 = < 0.10
G2–K0	1.3–1.4	1/25 = $0.04^{+0.08}_{-0.01}$	1/21 = $0.05^{+0.09}_{-0.02}$	1/25 = $0.04^{+0.08}_{-0.01}$	1/25 = $0.04^{+0.08}_{-0.01}$
K0–M0	0.7–1.3	6/67 = $0.09^{+0.05}_{-0.02}$	4/46 = $0.09^{+0.06}_{-0.03}$	8/68 = $0.12^{+0.05}_{-0.03}$	7/60 = $0.12^{+0.05}_{-0.03}$
M0–M4	0.2–0.7	35/231 = $0.15^{+0.03}_{-0.02}$	18/96 = $0.19^{+0.04}_{-0.04}$	41/210 = $0.20^{+0.03}_{-0.03}$	23/108 = $0.21^{+0.05}_{-0.03}$
M4–M8	0.035–0.2	97/387 = $0.25^{+0.02}_{-0.02}$	22/84 = $0.26^{+0.06}_{-0.04}$
M8–L2	0.01–0.035	4/23 = $0.17^{+0.11}_{-0.05}$
Debris and Evolved Transitional Disks					
B0–B8	2.8–18	0/25 = < 0.07	0/22 = < 0.08	0/25 = < 0.07	0/26 = < 0.07
B8–A6	1.8–2.8	0/45 = < 0.04	0/40 = < 0.04	5/46 = $0.11^{+0.06}_{-0.03}$	20/45 = $0.44^{+0.08}_{-0.06}$
A6–F4	1.5–1.8	1/20 = $0.05^{+0.10}_{-0.01}$	0/12 = < 0.13	3/21 = $0.14^{+0.11}_{-0.04}$	7/21 = $0.33^{+0.12}_{-0.08}$
F4–G2	1.4–1.5	0/18 = < 0.09	0/9 = < 0.17	0/18 = < 0.09	3/17 = $0.18^{+0.12}_{-0.06}$
G2–K0	1.3–1.4	0/25 = < 0.07	0/21 = < 0.08	1/25 = $0.04^{+0.08}_{-0.01}$	4/25 = $0.16^{+0.10}_{-0.05}$
K0–M0	0.7–1.3	0/67 = < 0.03	0/46 = < 0.04	0/68 = < 0.03	8/60 = $0.13^{+0.06}_{-0.03}$
M0–M4	0.2–0.7	0/231 = < 0.01	0/96 = < 0.02	0/210 = < 0.01	13/108 = $0.12^{+0.04}_{-0.02}$
M4–M8	0.035–0.2	0/387 = < 0.01	0/84 = < 0.02
M8–L2	0.01–0.035	0/23 = < 0.07

^a Masses that correspond to the given range of spectral types for an age of 11 Myr (Baraffe et al. 1998; Chabrier et al. 2000; Palla & Stahler 1999; Dotter et al. 2008; Pecaut et al. 2012).

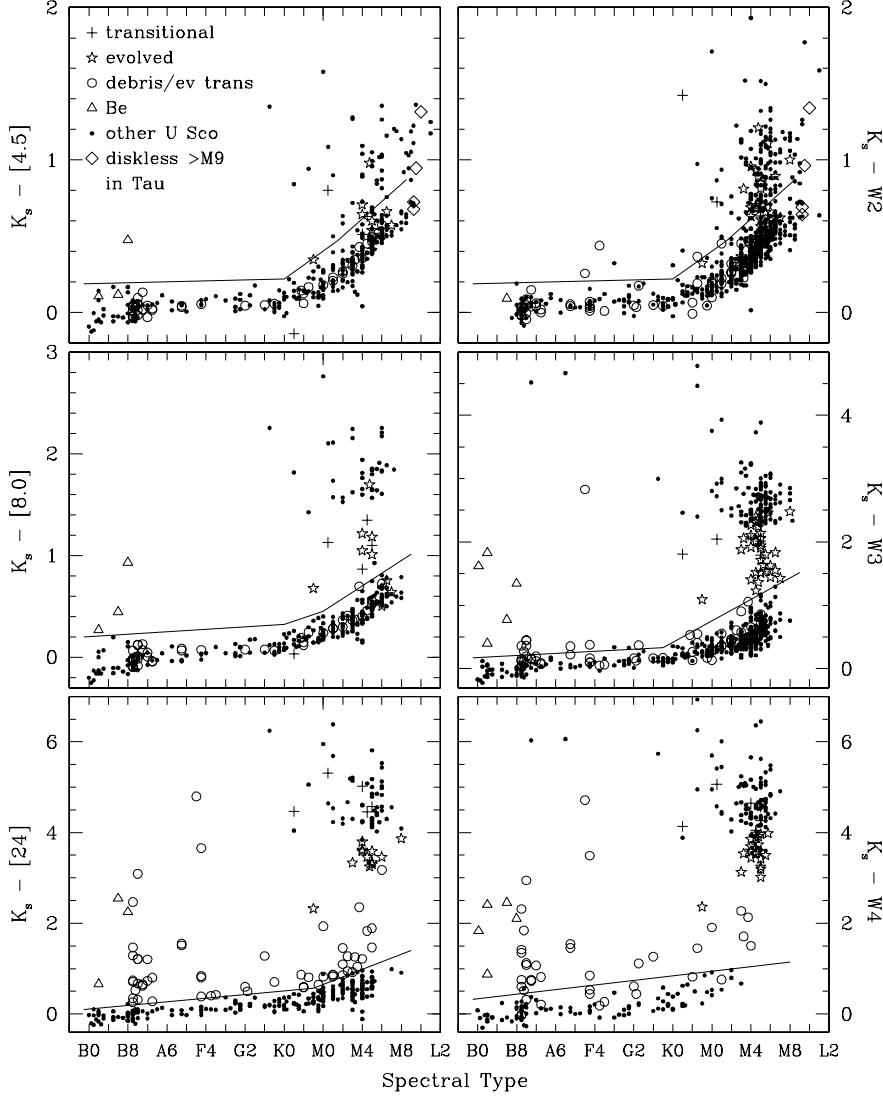


FIG. 1.— Infrared colors versus spectral type for members of Upper Sco based on data from *Spitzer* (left) and *WISE* (right). The solid lines are used to identify excess emission from circumstellar disks. For types later than M8.5, $4.5\ \mu\text{m}$ and W2 excesses are difficult to identify reliably because the photospheric colors increase rapidly, as shown by the data for Upper Sco and late-type diskless members of Taurus (diamonds). We have indicated known Be stars (triangles, Carpenter et al. 2009; Cieza et al. 2010) and candidates for transitional disks (crosses), evolved disks (stars), and debris or evolved transitional disks (circles, Carpenter et al. 2009; Chen et al. 2006, 2011, this work). Because the photospheric sequence is broader in $K_s - W4$ than $K_s - [24]$, some of the debris disk candidates at $24\ \mu\text{m}$ appear below the excess boundary for W4. Data at $24\ \mu\text{m}$ and W4 that have errors larger than 0.25 mag or that appear to be contaminated by extended emission are omitted.

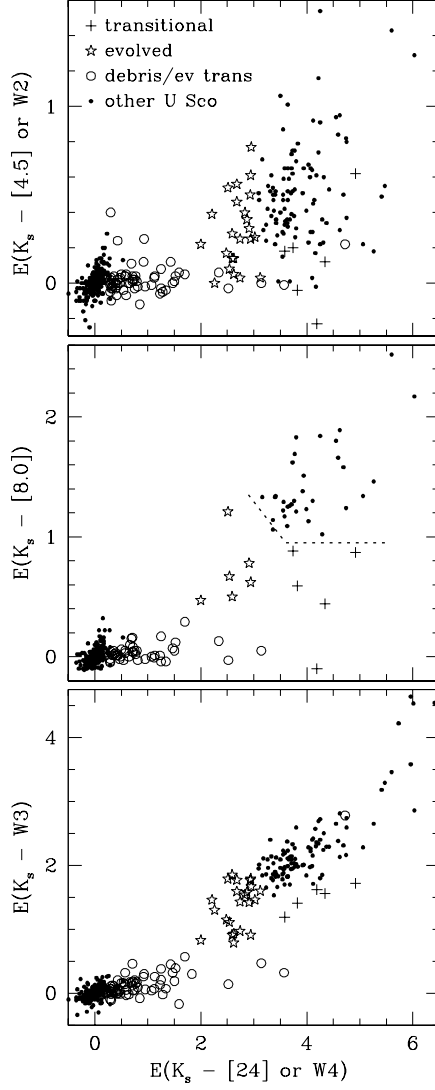


FIG. 2.— Infrared color excesses for members of Upper Sco. Data at 4.5 and 24 μm from *Spitzer* are shown when available. Otherwise, measurements at similar wavelengths from *WISE* are used (W2 and W4). We have indicated candidates for transitional disks (crosses), evolved disks (stars), and debris or evolved transitional disks (circles). In the middle diagram, we have marked the lower boundary that we have adopted for full disks (dotted line).

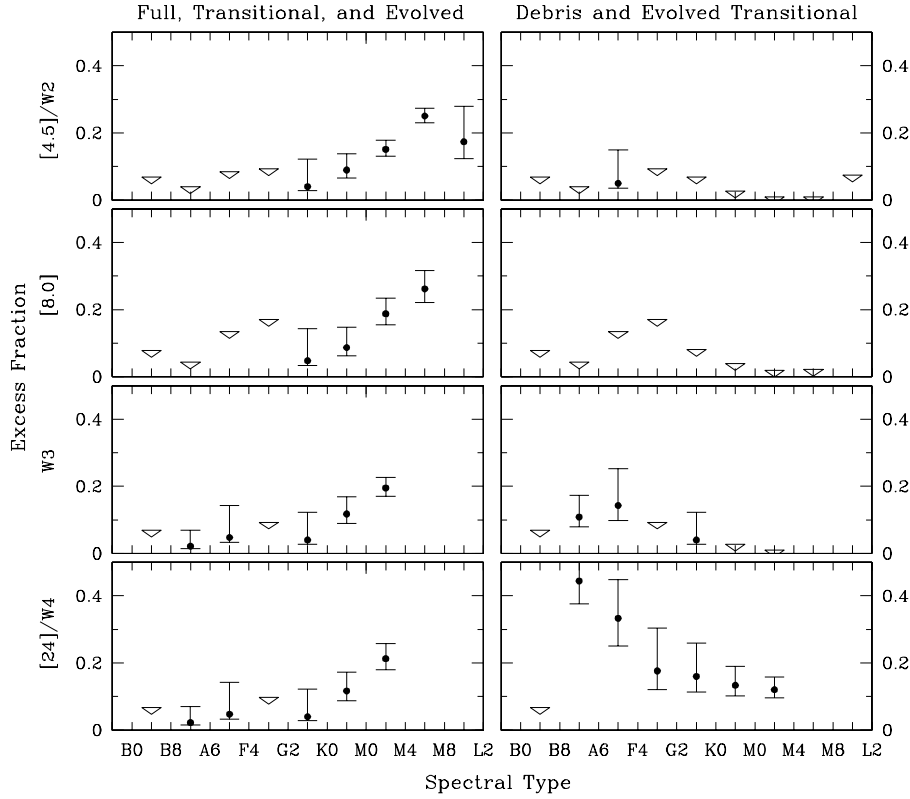


FIG. 3.— Excess fractions versus spectral type in Upper Sco for full, transitional, and evolved disks (left) and debris and evolved transitional disks (right, Table 2). For each band, data are shown only down to the coolest spectral type at which most of the known members are detected. The triangles represent 1σ upper limits.

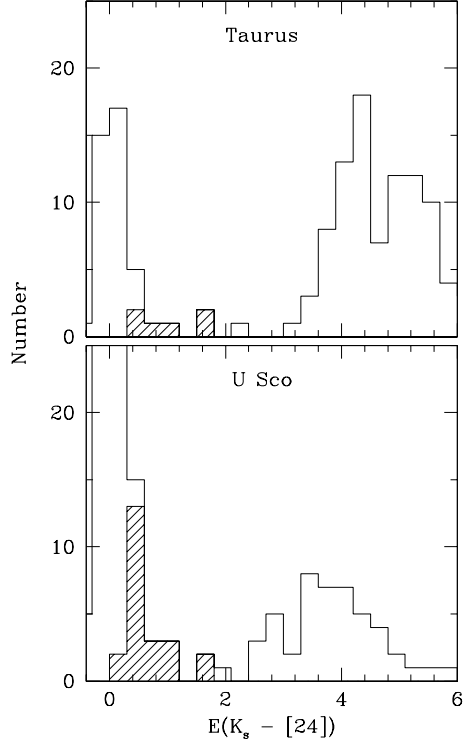


FIG. 4.— Distributions of $E(K_s - [24])$ for K0–M5 members of Taurus and Upper Sco. The shaded histograms represent stars that may have debris disks or evolved transitional disks based on their small $24\ \mu\text{m}$ excesses. Protostars have been omitted.